Effects of wave drag on submerged bodies

Influence des forces de traînée de la houle sur les corps immergés

Dr M. H. Abdul Khader

Faculty of Engineering
University of Singapore
Singapore 5

Introduction

When a deeply submerged body moves with a uniform velocity along a straight line through an unlimited fluid medium, it experiences a force in a direction opposite to that of motion. This force is called the drag or resistance. The same body will experience a larger drag when it moves near a free surface. The bodies moving near the free surface generate wave system on the surface by disturbing the interface. The increase in resistance is associated with the additional energy required to generate the wave system around the body.

The dimensionless force coefficients for submerged bodies, in incompressible fluids at large depths of immersion, are functions of the body geometry and Reynolds number. When the same bodies are moving at or near an interface between two fluids of different densities an additional energy is expended on the generation of interfacial wave system. In this case gravity influences the hydrodynamic flow field, and lift and drag forces on the body. An additional parameter Froude number has to be considered when gravity affects the flow field. In general the wave pattern around the body moving on or just beneath the free surface is complex, in particular for a three dimensional body.

Theoretical work

Since the beginning of this century, relatively few scientists and mathematicians have tried to formulate the wave resistance problems theoretically. In all their attempts, hydrodynamic conditions, i.e. the inviscid fluid conditions, were assumed. Havelock [1] developed the first order wave resistance theory for a submerged spheroid using the linearized free surface conditions. Wigley [2] simplified the Havelock's mathematical expressions and brought out the wave drag expressions into a convenient form. Recently, the second order wave resistance theory was developed and applied to a spheroid by Chey [3].

Experimental work

Much of the earlier work in studying the complex behaviour of the wave pattern developed around a three dimensional body when it is at or near the free surface was not successful. As a result only a meagre amount of experimental work was reported. And it was only after the development of first order wave theory, few experimental attempts were made for the simple cases like spheroids. Their objective was mainly the verification of the theoretical predictions. The experimental works carried out by Weinblum [4] and Bessho [7] were of considerable importance in this category.

Shortcomings of theoretical and experimental attempts

In all previous theoretical attempts the fluid was assumed to be inviscid and slip occurs on the body surface. Actually this is different from the real fluid condition. As was assumed earlier, the total drag on the body at the interface is not a simple summation of wave drag and viscous drag. As the wave drag and viscous drag interfere with each other, the theoretical results do not exactly concide with the experimental results, irrespective of the accuracy adopted in the experimental procedure. Present day mathematical knowledge is applicable for simple shapes of bodies like spheroids. Though the theory can be extended to all shapes of bodies, the limited mathematical tools available restrict its scope.

Experimental methods have their own drawbacks too. These methods are always limited to particular cases and it is not possible to study completely the

general behaviour of interfacial wave system. One of the serious drawbacks of the experimental studies is the interference of supporting mechanism with the flow field around the body, which adds an additional complexity to the problem.

Havelock [1] developed the first order wave resistance theory for a submerged spheroid, using the linearized free surface condition. For an infinitely deep submerged spheroid moving along the major axis at constant forward speed, the velocity potential may be expressed by distributed sources or doublets along the major axis of symmetry between the forward focus and aft focus.

From this body singularity he obtained the first order external velocity potential which consists of images in the upper half space. The complete first order velocity potential, which is the sum of the velocity potential for the first order body singularity and the first order external potential, satisfies the linearized free surface condition.

The importance of Wigley's [2] work lies in the approximations made in order to simplify the mathematical expressions derived by Havelock. Any solid of revolution can be represented by a line distribution of sources along its axis, while it is not easy to find the distribution appropriate to a given form, by successive trials of reasonable distributions.

The approximations made by Wigley was that the velocities in the free surface, induced by the motion of the body are so small compared to the speed of the body. The squares of the ratio between induced velocity at the free surface and the body velocity may be neglected. This assumption simplifies the boundary condition at the free surface, and it is then possible to find an expression for the velocity potential of a source in the presence of a free surface.

Wigley [2] presented numerical results in non-dimensional form for a spheroid. The parameters are coefficient of wave drag, Froude number and depth of submergence to length ratio f/l. The results are shown in Figure 1. It can be seen from the Figure 1 that the coefficient of wave drag increases rapidly upto the Froude number 0.5 and drops down in an exponential form after Froude number 0.55 onwards. Magnitude of wave drag increases as the f/l ratio decreases.

The first order velocity potential represents a flow

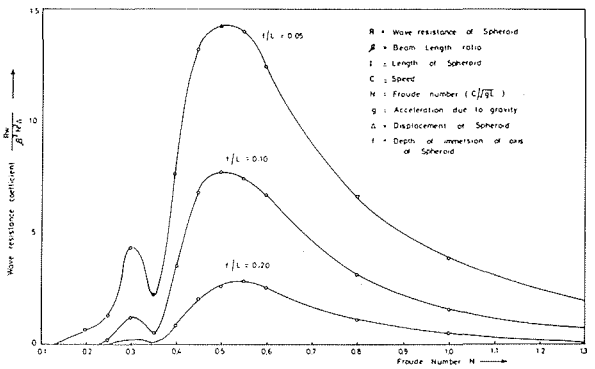

Figure 1 – The coefficient of wave resistance of a submerged spheroid.

about a distorted spheroid near the free surface. The spheroid is distorted because, when the induced velocity due to the first order external velocity potential is added vectorially to the flow velocity induced by the first order body singularity subjected to a uniform flow, the resultant flow velocity at the surface of the spheroid is no longer tangential to that surface. For the velocity potential to represent a flow about the original undisturbed spheroid, nonuniform strength of sources or doublets and nonlinear free surface conditions must be considered.

Chey [3] assumed nonlinear free surface condition and nonuniform distribution of sources, and formulated wave resistance equations for a spheroid. The contribution to the wave resistance from the second order body singularity and the nonlinear effect of the free surface condition decreases as the depth of submergence of the spheroid increases.

Weinblum [4], [5] conducted experiments on a spheroid model of length to diameter ratio 8 at Berlin towing tank. The model was 4.0 m long. The highest Froude number in the test was 0.4. The results showed that the free surface disturbance disappears at the depth of submergence to diameter ratio 4 to 5 for the slender spheroid.

Hughes [6] proposed a methodology for analysing the experimental data and to separate the wave resistance. This method, in effect, assumed that the viscous drag due to form effect at deep submergence is equal to that at a finite submergence. Strictly speaking, this is not true. The wavy pattern of the free surface is bound to influence the characteristics of the boundary layer. Also a thick boundary layer near the stern will definitely alter the surface wave shape in the vicinity of the stern. The interference effect between the boundary layer and the surface wave depends on the body shape as well as depth of submersion.

Bessho [7] in 1961 measured the resistance of a spheroid model of length to diameter ratio 8.06. The model was 2.4 m long. It was suspended by a strut which had an ogive cross-section with 11.78 cm chord and 1.78 cm thick.

Chey [3] conducted experiments on a spheroid with length to diameter ratio of 8. The length of the model was 1.42 m and the diameter at the mid section was 17.78 cm. The model was suspended by means of wires with diameter 0.078 cm. The drag on the body was measured by two drag balances fixed to a moving trolley.

The theoretical results evolved by first order wave theory ranges 10 % deviation at higher Froude number and at depths greater than body diameter. First order wave theory fails to predict the wave resistance on three dimensional axisymmetric bodies on the surface and just beneath the surface.

Experimental investigation

The objective of the experimental work is to study the behaviour of the free surface interference on the drag of three dimensional bodies. The bodies chosen are of two types.

(i) Ellipsoidal bodies of length 0.7 m, 1 m and 1.4 m $L/B = 7$.
(ii) Hydrodynamic body of length 0.4 m $L/B = 4$ and $L/C = 3$.

It is also the objective of the present experimental investigation to compare the experimental results of the above three ellipsoidal bodies with the analytical results of Wigley's [2] first order wave theory.

The experimental work is carried out in the Towing Tank of the Hydraulic Engineering Laboratory, Indian Institute of Technology, Madras.

Strut and body system

Preliminary experiments are conducted on the ellipsoid model of length 0.7 m. The model is fixed to the end of a streamlined strut of transverse length 0.2 m and thickness 0.02 m. The other end of the strut is fixed to a single component drag balance. Drag is measured at different depths of submergence for various velocities using the drag balance. The working of the drag balance is based on the strain gauge principle. This instrument is sensitive up to 12 grams and it can be used up to a horizontal force of 10 Kg. The following assumption is made in this approach.

The total drag measured on the body and the strut system is equal to the summation of the drag on the body and the drag on the strut measured individually. This in turn means that the flow field around the body and strut behaves independently. The two flow fields do not interfere with each other.

Experiments are conducted for drag at different depths and speeds. Experiments are repeated for the same depths, keeping the strut alone and the drag forces are measured without the body. Drag of the body for all the depths and speeds is separated from that of the combined system.

The following results are derived from the above experimental investigations.

(i) Drag coefficients of the strut when it is tested alone is found to be a function of aspect ratio (depth of submergence/strut transverse length). Drag per unit length of the strut decreases as the depth of submergence increases.
(ii) At larger depths of immersion, the percentage of drag on the strut is more in comparison to the body drag in the combined system.
(iii) At shallow submergence, drag on the strut includes the wave effect caused by the body.

The above observations reveal that the combined behaviour of body and strut is a complex phenomena. The drag coefficients calculated for the body are found to be irregular. The drag on the strut at the free surface in the combined system includes the wave effect which is a considerable quantity.

Shear casing around the strut

This method includes the improvements made to avoid the strut behaviour from the measuring system. An aluminium cover is made around the strut leaving a gap of 2 mm on the periphery of the strut. This aluminium casing covers the strut and takes the forces coming on to the strut. This casing is separately connected to the trolley so that the forces coming on to the shear casing is transfered to the trolley independently. The assumption involved in this approach is that the drag recorded by the drag balance is that of the body only. The interesting result obtained in this investigation is that the drag observed on the body for a constant depth of immersion changes with the position of shear casing. A decrease in drag is observed when the shear casing is moving away from the body. Actually this should cause an increase in drag involved due to the additional projection of strut in the measurement. The decrease is observed only for a certain distance of shear casing, afterwards an increase is observed. From these observations it can be concluded that the body drag is effected by the shear cover, causing an interference with the flow field around the body.

Wire suspension mechanism

To avoid the complications caused by the strut mechanism, completely a different method is tried in which the body is suspended by wires. To overcome the buoyancy forces, heavy loads are inserted within the bodies. The wires are kept in tension when the bodies are under water. Two wires are connected to each end of the model forming "V" shape. The other ends of the wires are fixed to a sliding frame. Sliding frame is connected to a two component drag balance. When the trolley is in motion, the drag force experienced by the body moves the sliding frame. The movement of the frame is arrested by balancing it with weights. The advantage of this method is in the replacement of strut by very thin wires (0.7 mm dia) whose interference with the flow around the body is negligibly small.

Preparation of the models

The ellipsoidal models of length 0.7 m, 1 m and 1.4 m, and the hydrodynamic body of length 0.4 m are made of wood. Additional weights are necessary to maintain the models' negative buoyancy during the experiment. To avoid the heeling effect of the body in the axial motion, weights are added along a single line normal to the centroidal axis. Added weights are symmetric about central transverse plane. Radial drills are made on the body along a single line parallel to the centroidal axis. The depth of the holes are maintained same for the holes equidistant from the mid-transverse section. Molten lead is poured into the holes. After solidification of the molten lead, the holes are packed with wood. Smooth surface finish is given with sand paper.

Dynamic force balance

A dynamic force balance, which is a mechanical system, is designed and fabricated exclusively to measure the drag forces on the bodies under investigation. The main objective of this instrument is to work sensitively for the range of forces from 50 grams to 4 000 grams,

within an accuracy of less than one percent. The instrument is provided with an adjustable wire fixing arrangement (Fig. 2). The depth of submergence of the suspended bodies can be adjusted as per the requirement with the above wire fixing arrangement. The balance consists of a fixed frame and a movable frame. The above two frames are hinges by two suspension frames. A balancing beam is provided at the centre of the instrument. The balancing beam is hinged to the moving frame as well as the fixed frame. An indicator is fixed to the free end of the balancing beam. A counter needle is also provided to magnify the deflection of the balancing beam. When the body is in axial motion, the resistance on the body will be transfered to the movable frame. This in turn moves the central balancing beam.

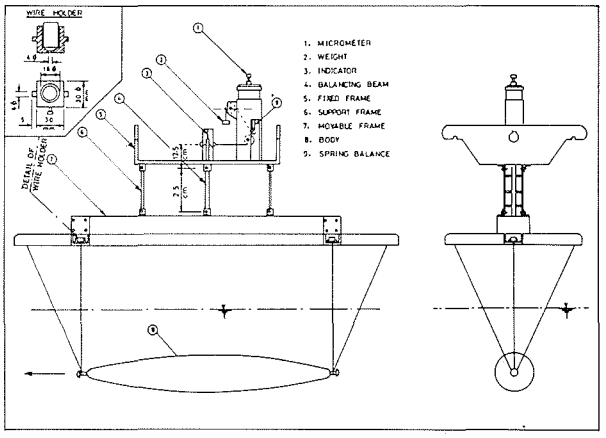

Figure 2 – Dynamic force balance.

Experimental procedure

Models are suspended to the movable frame of the dynamic force balance. Depth of immersion of the body at the forward and aft ends of the body are checked to be the same for every depth. The models are checked for longitudinal alignment with reference to the trolley.

The important measurements involved in these experiments are :

(i) Drag on the models,
(ii) Velocity of the carriage,
(iii) Depth of submergence of the model, and
(iv) Temperature of the tank water.

Drag on the model is measured by suspending weights and creating tension in the spring balance by operating the micrometer head.

Experimental results

Drag tests are conducted on three ellipsoidal models of length 0.7 m, 1 m and 1.4 m and one hydrodynamic body of length 0.4 m. These tests are conducted in the velocity range of 1 m/sec to 2.5 m/sec. For velocities greater than 2.5 m/sec, sagging effect is observed on the suspended wires and the bodies are found to be unstable during their course of run. Maximum free surface disturbance in the case of ellipsoids is observed for velocities corresponding to the Froude number ($F_n = V/\sqrt{gL}$ where V is the velocity of the body and L is the length of the body) 0.5.

The drag values for 1.4 m and 1.0 m ellipsoidal models are obtained by subtracting the calculated values of drag on the wires. (The drag on the wires are calculated assuming the coefficient of drag equal to 1.19 for Reynolds number of 1×10^4. The values of total drag coefficient $C_T(R_T/1/2\,\rho A V^2$ where R_T is the total drag on the body, ρ is the density of the fluid, A is the surface area of the body and V is the velocity of the body, are calculated). The C_T values are plotted to a base of Froude number, for various f/b ratios (f = depth of immersion of the centroidal axis and b = maximum diameter of the body) and are shown in Figures 3, 4, 5 and 6. From these figures, cross curves are drawn showing the variation of total drag coefficient with f/b ratio

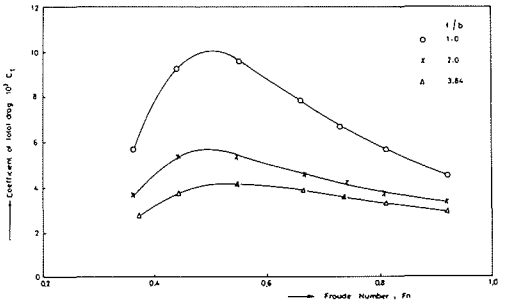

Figure 3 – Specific total drag curves for ellipsoid 0.7 m model.

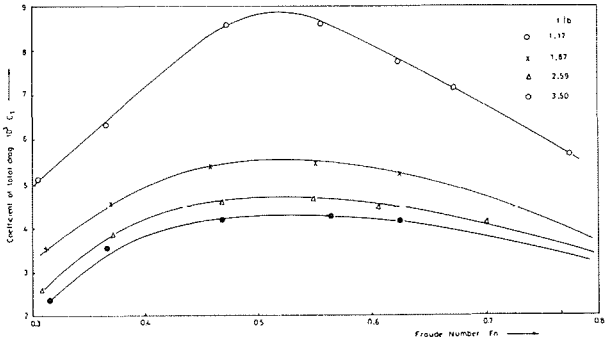

Figure 4 – Specific total drag curves for ellipsoid 1.0 m model.

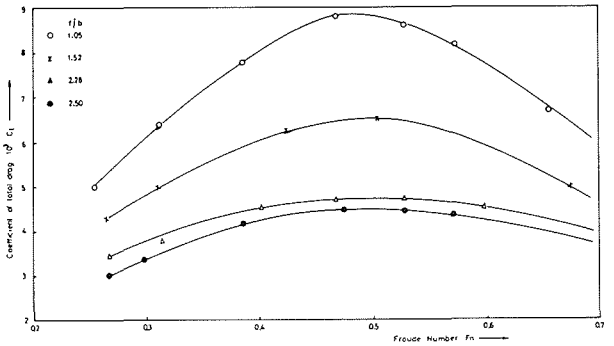

Figure 5 – Specific total drag curves for ellipsoid 1.4 m model.

for constant Froude numbers and are shown in Figures 7, 8, 9 and 10. All these curves show that C_T rapidly decreases up to f/b ratio equal to 4, and later the curves are asymptotic.

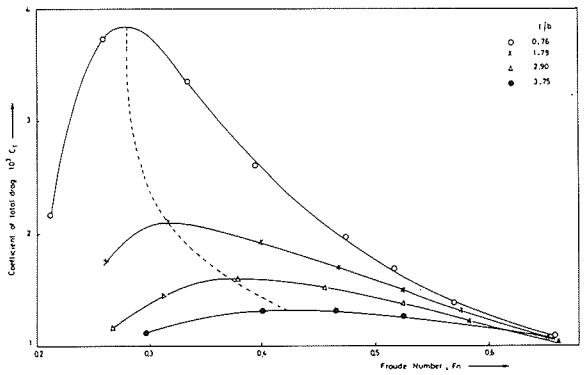

Figure 6 – Specific total drag curves for 0.4 m hydro-dynamic body.

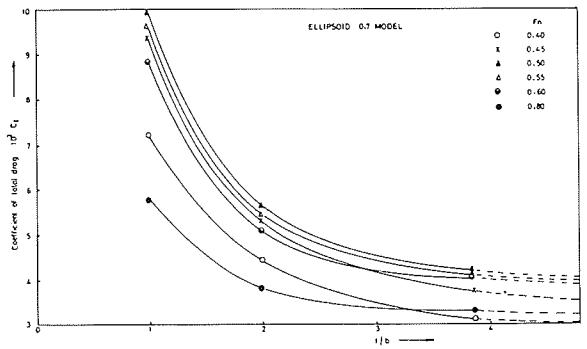

Figure 7 – Variation of specific total drag with f/b.

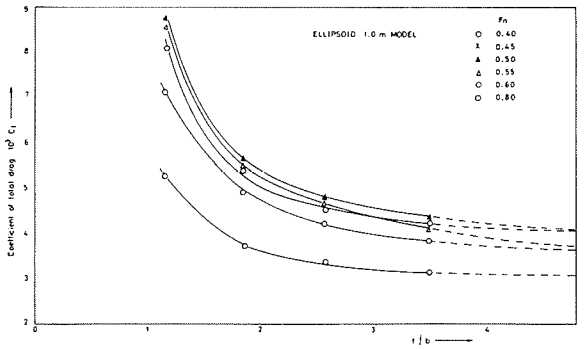

Figure 8 – Variation of specific total drag with f/b.

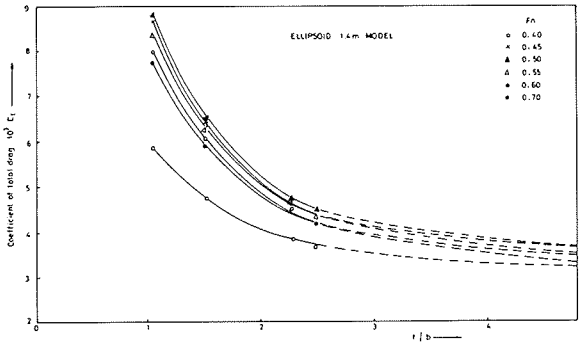

Figure 9 – Variation of specific total drag with f/b.

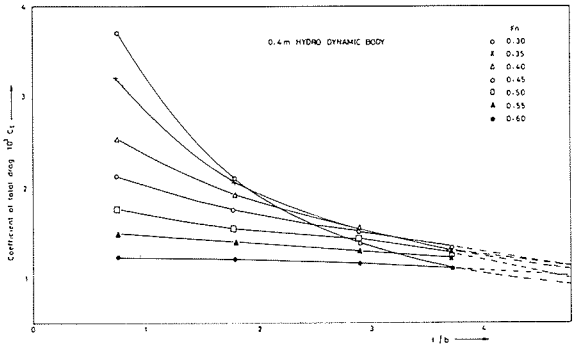

Figure 10 – Variation of specific total drag with f/b.

The following assumptions are made in the subsequent analysis of the experimental results.

(i) $C_T = C_V + C_w$ i.e.
The total drag coefficient is equal to the sum of viscous drag coefficient,
$C_V \left(= \dfrac{R_V}{1/2\ \rho A\ V^2}\right)$, and wave drag coefficient,
$C_w \left(= \dfrac{R_w}{1/2\ \rho A\ V^2}\right)$, where R_V and R_w are the viscous drag and wave drags respectively.

(ii) The asymptotic values of drag coefficients at $f/b = 4.5$ are taken as the viscous drag coefficients in conformity with the work of Weinblum [4].

Discussion of the experimental results

From the Figures 6, 7 and 8 it can be seen that the coefficient of wave drag increases with the Froude number up to a value of 0.5, for depths of immersion f/b less than 4. It attains a maximum value in the Froude number range of 0.5 to 0.55, and starts falling thereafter. This behaviour is independent of depth of submergence. The total drag coefficient with free surface interference attains a maximum value for a particular Froude number.

A very interesting and important result is observed in the case of Hydrodynamic body. This body is not symmetric about the mid section, and the length to maximum diameter ratio is 4, maximum diameter is at 1/3 of the length. From the Figure 9 it can be seen that the maximum free surface disturbance for different depths of immersion do not occur at a single value of Froude number. Maximum wave effect on the body depends upon Froude number as well as depth of immersion.

Comparison of theoretical and experimental values

From Figures 11, 12 and 13 it can be seen that the theoretical and experimental values of the wave drag agree well at higher Froude numbers. In the Froude number range 0.4 to 0.8 for a given f/b value, as the model size increases the deviation of the experimental values from the theoretical values is less. At lower Froude number 0.4 the deviation is nearly 80 %. At Froude number 0.6 the deviation is between 8 % and 24 %.

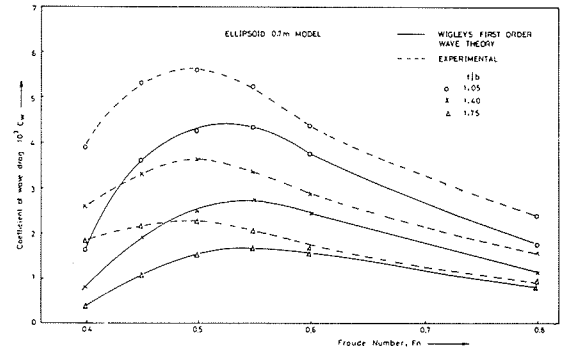

Figure 11 – Variation of specific wave drag with Froude number.

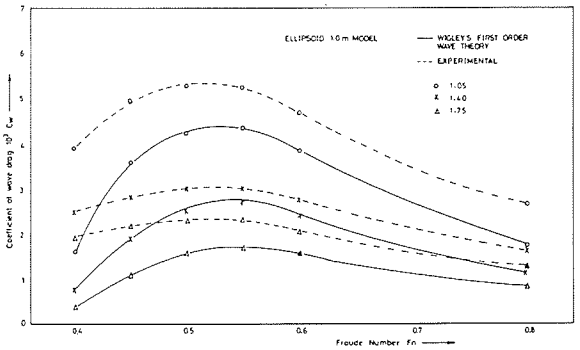

Figure 12 – Variation of specific wave drag with Froude number.

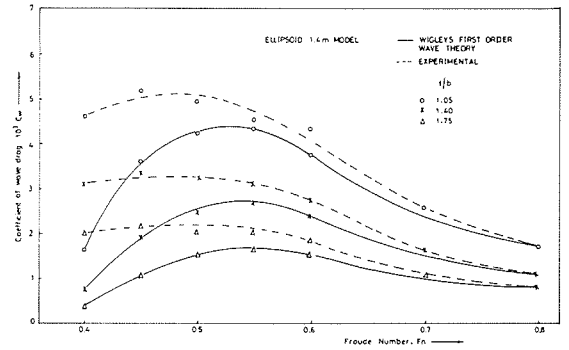

Figure 13 – Variation of specific wave drag with Froude number.

Conclusions

1) For the bodies axisymmetric and symmetric about mid section having length to beam ratio 7, maximum wave effect for all depths of immersion occurs in between Froude numbers 0.5 and 0.55.

2) As the length to beam ratio decreases, maximum wave effect occurs at lower Froude numbers.

3) For axisymmetric bodies which are not symmetric about mid transverse section position of maximum wave effect changes with depth of immersion.

4) For all axisymmetric bodies, free surface wave effect becomes negligible for depths of immersion greater than four times the maximum diameter of the body.

5) Interface wave effect is a function of $1/b$ ratio, shape of the body, f/b ratio and Froude number.

Acknowledgement

The experiments were carried out by Mr. P.V. Rao under the supervision of the author.

References

[1] HAVELOCK T.H. – The wave resistance of a spheroid, *Proceedings of Royal Society*, London, Series A, Vol. 131, 1931, pp. 275-285.

[2] WIGLEY W.C.S. – Water forces on submerged bodies in motion, *Transaction of Institute of Naval Architects*, 1953, Vol. 95, p. 268.

[3] CHEY YOUNG H. – The consistent second order wave theory and its application to a submerged spheroid, *Journal of Ship Research*, March 1970.

[4] WEINBLUM G.P., AMTSBERG H. and BOCK W. – Tests on wave resistance of immersed bodies of revolution, *DTMB translated print*, 234, 1950.

[5] WEINBLUM G.P. – The wave resistance of bodies of revolution, *DTMB report*, 758, 1951.

[6] HUGHES G. – Friction and form resistance in turbulent flow, and a proposed formulation for use in model and ship correlation, *Transactions of Institute of Naval Architects*, 1954.

[7] BESSHO M. – Wave resistance of submerged bodies of revolution, *Defence Academy*, Japan, 1961.